Serrano, J.; Arnau Martínez, FJ.; García-Cuevas González, LM.; Gómez-Vilanova, A.; Guilain, S.; Batard, S. (2021). A Methodology for Measuring Turbocharger Adiabatic Maps in a Gas-Stand and Its Usage for Calibrating Control Oriented and One-Dimensional Models at Early ICE Design Stages. Journal of Energy Resources Technology. 143(4):042303-1-042303-11. https://doi.org/10.1115/1.4048229

A METHODOLOGY FOR MEASURING TURBOCHARGER ADIABATIC MAPS IN A GAS-STAND AND ITS USAGE FOR CALIBRATING CONTROL ORIENTED AND 1D MODELS AT EARLY ICE DESIGN STAGES

José Ramón Serrano[1]
CMT-Motores Térmicos
Universitat Politècnica de València
Valencia 46022, Spain.
Email: jrserran@mot.upv.es

Francisco José Arnau
CMT-Motores Térmicos
Universitat Politècnica de València
Valencia 46022, Spain.
Email: farnau@mot.upv.es

Luis Miguel García-Cuevas
CMT-Motores Térmicos
Universitat Politècnica de València
Valencia 46022, Spain.
Email: luiga12@mot.upv.es

Alejandro Gómez-Vilanova
CMT-Motores Térmicos
Universitat Politècnica de València
Valencia 46022, Spain.
Email: algovi2@mot.upv.es

Stephane Guilain
Renault Nissan Mitsubishi
1 Allée Cornuel Lardy 91510, France
Email: stephane.guilain@renault.com

Samuel Batard
Renault Group
1 Allée Cornuel Lardy 91510, France
Email: samuel.batard@renault.com

[1] Corresponding author information can be added as a footnote.

ABSTRACT

In this work it is proposed a methodology to standardize turbochargers testing based in measuring the maps twice: in close to adiabatic and in diathermal conditions. Along the paper it is discussed with special detail the impact of the procedure followed to achieve said quasi-adiabatic conditions in both the energy balance of the turbocharger and the testing complexity. As a conclusion, the paper proposes a methodology which combines quasi-adiabatic tests (cold and hot gas flow) with diathermal tests (hot gas flow) in order to extract from a turbocharger gas-stand all information needed by engine designers interested in controlling or 1D-modelling the ICE.

The methodology is completed with a guide for calibrating said control-oriented turbocharger models in order to separate aerodynamic efficiency (adiabatic) from heat transfer losses and from friction losses in the analysis of the turbocharger performance. The outsourced calibration of the turbocharger model allows avoiding uncertainties in the global ICE model calibration, what is very interesting for turbochargers benchmarking at early ICE-turbo matching stages or for global system analysis at early control design stages.

1. INTRODUCTION

As new pollutant emissions and fuel consumption regulations become more severe, it also becomes necessary a deeper degree of charging at the ICE. Some evidences of the previous, are the several studies dealing with new technologies in the context of turbocharging the ICE. Some examples of the previous are: Ball bearings technology [1]; two stage turbocharging [2,3]; SRCT usage [4,5] and twin entry turbines [6].

Traditionally, spark ignition engines have been turbocharged by means of Waste-Gate turbines. The operative principle of these turbochargers, as its name suggests, is to by-pass the turbine as a function of the engine boosting requirements. Inherently, by-passing the turbine is a synonym of wasting the available energy in the exhaust gases.

However, due to new material technologies, VGT implementation becomes a potential upgrade for gasoline direct injection engines. The main benefit of the VGT technology, is the turbine-engine better matching through the wide engine operative conditions [7]. The higher efficiency of the turbine goes hand in hand with lower engine backpressure. It is a fact that exhaust gasses in gasoline engines are hotter than in diesel ones. This is mainly due to the stoichiometric mixture requirements for after-treatment operation. In consequence, active turbocharger cooling for VGT thermal protection becomes a must. Furthermore, a proper thermal barrier between the oil and the turbine side is necessary for oil-coking prevention.

In previous studies, heat transfer role has been deeply discussed [8–10]. Because of typically higher exhaust temperatures in gasoline engines and the usage of coolant, it can be expected that thermal gradients taking place in gasoline application turbochargers would be higher, leading to higher heat fluxes between the several turbocharger elements. In this line, proper estimation of the heat transfer phenomena may be even more necessary for accurate simulations.

In this study, three actively cooled, new generation VGT turbines for gasoline engine application, have been tested in a gas stand. Tests have been performed in several conditions: Almost-adiabatic, hot exposed and hot insulated. Careful management and selection of the recorded data has been carried out as it is reflected in the “Experimental campaign” section. Moreover a careful energy balance study has been performed to evaluate the quality of the recorded information. All the possible energy fluxes have been taken into account.

In combination with the previous, geometrical properties were measured (if possible), or estimated (since disassembling was not an option). The aforementioned geometrical parameters, are required by the heat transfer [11,12] and mechanical losses models [13], for heat and friction computation.

Having collected all the previous information, an iterative procedure gave as a result purely adiabatic maps. The iterative procedure is detailed in the "Modeling stage" section. From the previously mentioned procedure, a calibrated Heat Transfer and Mechanical Losses Turbocharger Model (HT-ML-TCM) has been obtained for all three turbochargers as well.

Later, turbo1 was assembled in a gasoline EU6 engine. In addition, after having obtained validated sets of turbocharger maps and a well-calibrated HT-ML-TCM: GT-POWER simulations were performed (also for turbo1). This way, a final procedure validation is carried out in engine context. Experimental collected data and modeling results have been compared.

Finally, a second set of simulations were performed without coolant into the turbocharger. Results were analyzed and the influence of the water usage in turbocharger for gasoline engine application is assessed.

2. EXPERIMENTAL CAMPAIGN

The testing campaign has been carried out in the gas stand described in [12]. The followed strategy for the three VGT turbocharger units is the one described in this section.

In a first stage, almost-adiabatic maps were recorded. These maps are obtained under a methodology that allows for severe heat transfer reduction. The full turbocharger is insulated and no cooling water is employed. In the same line, compressor air, turbine gas and lubricating oil were kept as similar as possible. The last is necessary to minimize internal heat fluxes between the several heat sinks/sources. Fig. 1 shows the gas stand test bench under insulated working conditions configuration.

There are several approaches in the available literature for heat transfer accounting. One of the approaches consists on fluids mean working temperatures as the temperatures used for heat transfer estimation. Other approaches suggest that the compressor outlet, turbine inlet and oil inlet temperatures should be the ones selected. In other words, depending on the approach followed, if heat transfer in the turbocharger is aimed to be reduced during tests:

- Compressor, oil and turbine mean temperatures are to be kept as similar as possible. This is the selected approach for turbo2.
- Compressor outlet, oil inlet and turbine outlet temperatures are the selected variables to be kept as similar as possible. Fig. 3 (A) is a good example of this approach (turbo1). Turbo3 also followed this strategy.

It was decided that, for proper adiabatization, 10 ºC was the maximum temperature difference between the fluids. This temperature difference presented a good compromise between testing-time-consumption and heat reduction. Regardless of the selected strategy for almost-adiabatic measurements, the target was to stabilize the

monitored temperatures as close as possible to the desired target. Some safety issues were kept in mind during these tests:

- Oil temperature was adjusted within a range of 35-110 ºC. For some working points, i.e. very high compressor pressure ratios oil heating would be excessive (for proper adiabatization). However, because of oil coking and lubricating properties losses, it was not exceeded the aforementioned range. In “Modeling stage”, the heat transfer model copes with the residual heat fluxes arising. This way, purely adiabatic maps can be expected. Thus experimental campaign limitations are solved.
- Minimum turbine inlet temperature was controlled in order to avoid water condensation. In the test bench, the software calculated on-live the dew temperature. Turbine outlet temperature was always kept above.
- Pressure difference between the compressor outlet and turbine inlet. Axial forces that arise as consequence of “pressure time’s wheel area differences” between the compressor and turbine should be limited. By general rule 1.5 bar was the maximum accepted pressure difference. This point was of high importance during almost-adiabatic measurements, since much higher turbine inlet pressure was required. Fig. 3 (C) shows the pressure differences along the rotational speed recorded range.

No water was employed in almost-adiabatic tests, in order to avoid extra heat sinks/sources.

The temperatures for each recorded point were set up by means of several PID in the gas stand. All the temperatures were registered from two to four times, depending on the space available, i.e., the compressor inlet and outlet temperatures were registered by four thermocouples. All pressures were recorded by two sensors (in the same socket). In the particular case of the turbine inlet temperature, and due to space constraints, only one sensor was assembled. However, for checking purposes, stagnation temperature in a small tank upstream the exhaust manifold inlet (turbine inlet) was also installed.

Mass flows were recorded twice (inlet and outlet) for leakages or infiltration issues detection. Fig. 3 (B) shows compressor inlet and outlet mass flows. Fig. 3 (D) shows the same information for the turbine. As it is shown, for the lowest mass flows, the range of one of the sensors was exceeded. In these cases, the average between both sensors was not performed.

Furthermore, lubricating oil temperature and mass flow were additionally recorded. For all the experimental campaign, standard thermal stabilization criteria [14] was followed. Temperatures variation rate was ensured to be lower than 0.5 ºC / min before the recording. For this study, since heat transfer was one of the phenomena to be analyzed, wall temperatures were also recorded. Three wall thermocouples were installed in several location: Turbine volute and backplate, central housing and compressor backplate and volute.

For hot insulated/exposed cases, the major time-consuming aspect corresponded to the thermal stabilization criteria for steadiness assurance. On the one

hand, hot insulated test were performed to avoid external heat transfer. On the other hand, exposed tests allowed for external heat fluxes. In the case of the exposed ones, environmental conditions such as surrounding air velocity and temperature were monitored in order to perform a proper "calibration" of the external heat transfer model. For both test types, water inlet/outlet temperatures were recorded. Water mass flow was recorded as well. Fig. 2 shows the same gas stand, for exposed conditions tests.

As final validation of the recorded data quality, an energy balance was performed. Fig. 4 shows the energy balance for all three turbocharger units. Unbalance was calculated according to Eq. 1). The terms that enable for the energy unbalance balance are: "$\dot{W}_{\mathrm{oil}}$", "$\dot{W}_{\mathrm{water}}$", "$\dot{W}_{\mathrm{turb}}$" and "$\dot{W}_{\mathrm{comp}}$". The aforementioned terms are calculated directly as mean mass flow rates times the temperature difference between inlet and outlet. Turbine and compressor external heat transfer become the main reasons why a high unbalance arises for hot exposed tests (since external heat transfer is not recorded, neither added to the energy balance). Unbalance higher values reach values up to 89 %. In other words, external heat transfer is the governing phenomena for the low power working points.

As it could have been expected, an almost perfect balance is obtained from the almost-adiabatic tests for all three turbocharger units. This is possible, since external heat transfer (the only un-accounted variable), has been diminished as much as possible.

The “non-perfect” insulation could explain the slightly un-equilibrated energy balance in the hot insulated tests for turbo1. On the contrary, turbo2, hot insulated tests, result in a “negative” energy balance. In other words, working conditions stated in Eq. (2) is taking place. This is attributed to the heaters over-reaction during the the thermal transient for the turbine inlet temperature accomplishment. In other words, this transient, prior to the steady state is mainly governed by the system inertia and the e-heaters PID. Even if the turbine inlet temperature was stabilized, the insulation material and the turbocharger metal itself accumulated some heat during the thermal transient prior to the steady state. Later, the aforementioned accumulated heat was slowly released to lower temperature fluids: water, oil and compressed air. Consequently, these fluids’ outlet temperatures were affected (slightly hotter than it should), leading to the observed “negative energy balance”. For the turbo3 it was not performed any hot insulated test campaign.

Fig. 5 compared for all three turbocharger units the energy balance results from the almost-adiabatic tests. The mean unbalance for turbo2 is the one closest to zero. It should be recalled here that only for turbo2 the stabilization criteria was the one that considered the mean fluids working temperatures. This criterion is the one that takes more time to stabilize, since turbine and oil outlet are being considered for the thermal stabilization. Thus, if the recorded data is aimed to be directly used for turbocharger aerodynamic maps generation, mean working fluids temperatures should be included in the stabilization criteria.

$$\text{Unbalance} = (\dot{W}_{\text{water}} + \dot{W}_{\text{oil}} + \dot{W}_{\text{comp}})/\dot{W}_{\text{turb}} \cdot 100 \quad (1)$$

$$\dot{W}_{\text{water}} + \dot{W}_{\text{oil}} + \dot{W}_{\text{comp}} > \dot{W}_{\text{turb}} \quad (2)$$

3. MODELING STAGE

Colors criteria have been fixed to any forward turbocharger plot/comparison. Table 1 shows the selected color-speed ranges for each iso-speed range. From this section in advance, any turbine map will follow the criteria described in Table 1.

The CMT-TCM is the one selected for the complete modeling of the three studied turbochargers. This model makes usage of basic geometrical data in combination with physical and semi-empirical equations. At the same time, the model is constituted by two sub-models:

- Heat Transfer & Mechanical Losses model (HT-ML): The model copes with any heat flux that takes place (internal conduction, internal/external convection and radiation). Friction losses are also estimated. The friction losses model computes the friction power in both, the radial and thrust bearings. In all, the HT-ML model subtracts the heat and friction losses from the effective turbocharger efficiency (ETE), coming from the experimental campaign. ETE definition is shown in Eq. (3).

  As a result, purely adiabatic points become the model output. In Fig. 6 according to the previous, it is shown how from ETE the model obtained for each point, the adiabatic efficiency. The model decouples the More details can be found in [15].

$$ETE = \dot{W}_{\text{comp}}/\dot{W}_{ISENTROPIC\_turb} \quad (3)$$

- Turbine and compressor maps model: A series of parameters are adjusted to fit the purely adiabatic data and obtain the so-called extrapolated turbine and compressor aerodynamic maps. This fitting is performed for the mass flow and efficiency as explained in [16,17]. The result for this fitting is shown in Fig. 6.

Having described the model capabilities and having collected the previously described experimental information, the model calibration procedure can be summarized in the diagram of Fig. 7. One of the major benefits of the proposed methodology lies in the fact that the different phenomena can be decoupled from the rest. This allows for aerodynamic maps, mechanical losses and heat transfer models semi-independent calibration. As it can be deducted from diagram in Fig. 7, step by step, each of the model variables prediction is compared against the experimental data. Until the adjustment is satisfactory, the loop is repeated (red rows). Finally, when the quality of the variable prediction is accepted: Green lines show the next step to follow and the calibration of next turbocharger "sub-model" begins. Before starting with the calibration procedure, it is of high importance checking the quality of the fitted maps in terms of mass-flow.

According to the diagram in Fig. 7 thanks to the adiabatic campaign, heat transfer to the oil was minimized: The major raise of oil enthalpy, can be attributed to the mechanical losses. Presumably, any disagreement between the model results and the experimental data comes from the mechanical losses model "K_{jb}". Parameter "K_{jb}" is the one to be adjusted in Eq. (4). As it can be understood from equation Eq. (4),

mechanical losses power "$\dot{W}_{jb}$" also depends on the bearing geometry, oil properties and mean conditions as well as TC speed.

Once the mechanical losses model has been calibrated, internal heat transfer model can be adjusted without the uncertainty of the external heat losses (as far as hot external insulated test campaign had been carried out). The calibration of the internal conductances, guarantees a good prediction of internal heat transfer. The term of internal conductance is represented by "$K_{\mathrm{i}-(1+1)}$" in Eq. (5) for metal nodes heat power calculation "$\dot{Q}^{cond}_{i-(i+1)}$". As it is shown in equation Eq. (5), metal nodes heat power also depends on the temperature difference between two consecutive nodes: "$(T_i - T_{\mathrm{i}+1})$". An example could be the temperature difference between the compressor backplate and the housing.

The final step corresponds to the external heat transfer model calibration. At this point, model-to-experimental data discrepancies are attributed to the external heat transfer model (since all previous models have been validated). The iterative loop (red row number 9 in Fig. 7) is repeated until a good solution is achieved.

This step is evidenced in Eq. (6), where "A_{i}" represents the external surface or area of the element "i". The elements in which the external surface is thermally divided are: Compressor case, central housing and turbine volute. In Eq. (6), the term "$h_{\mathrm{i}-\mathrm{ext}}$" represents the external convective coefficient. The model automatically estimates whether natural or forced convection is taking place. According to the previous "$h_{\mathrm{i}-\mathrm{ext}}$" is calculated as a function of the surroundings air velocity.

$$\dot{W}_{jb} = 2\,\pi\,R_{jb}^{3} K_{jb} \frac{L_{jb}}{h_{jb}} \mu\left(\overline{T_{\mathrm{oil}}}\right) n^{2} \tag{4}$$

$$\dot{Q}_{i-(i+1)}^{cond} = K_{\mathrm{i}-(1+1)}(T_i - T_{\mathrm{i}+1}) \tag{5}$$

$$\dot{Q}_{i-ext}^{conv} = A_{\mathrm{i}}\, h_{\mathrm{i-ext}}\, (T_{\mathrm{ext}} - T_{\mathrm{i}})\ \mathrm{HTM} \tag{6}$$

4. RESULTS FROM TURBOCHARGERS' GAS STAND MODELLING

It is of high importance, the quality of the obtained maps during the model fitting procedure. Table 2 gathers the mean square root error committed during the adjustment for all three turbines. Errors during the fitting procedure do not reach 1% error in terms of mass flow and adiabatic efficiency adjustment. This check would correspond to box three in the diagram of Fig. 7.

The obtained maps for turbo1 are shown in Fig. 8. Only three VGT positions have been chosen for in Fig. 8 (A) in order to ease the view of the fitting. Figure 8 (A) deals with mas flow maps (in reduced units). Fig. 8 (B) corresponds to the turbine adiabatic efficiency map. The model automatically extrapolates the maps in a wide range of pressure ratio. This is highly useful for ICE turbocharger maps application.

Wall temperature analysis is shown in Fig. 9 for two VGT positions in Turbo1 and hot exposed cases. Good agreement between model and experimental has been achieved. Wall temperature distribution is a good indicator of proper heat fluxes estimation. In Fig. 9 "TN" represents Turbine Node, "H1" represents Housing 1 and so on. "TI" and "CO" correspond to Turbine Inlet and Compressor Outlet fluids respectively. The predicted wall temperature is an output of the complete model: Heat fluxes arising from the metal-to-fluids temperature differences, imply metal temperature gradients.

The last, in combination with metal nodes conductance's, allows to predict the wall temperature distribution along the turbocharger (from turbine volute to compressor case), as it is shown in Fig. 9.

To show an example of the final model accuracy, hot exposed results are shown for Turbo1 in Fig. 10. During the gas stand simulations, inlet conditions and rotational speed were imposed. The error in turbine and compressor outlet temperatures are always within ±3 %. Turbine corresponds to Fig. 10 (A) and compressor to Fig. 10 (D).

If mass flow maps had not been fitted previously, a wrong output of the mass flow for a given pressure ratio would have resulted. The highly accurate prediction of the oil friction losses power is noticeable in Fig. 10 (C). In these cases, oil enthalpy increase results from heat transfer and mechanical losses. Since mechanical losses had previously been validated for the adiabatic tests, just heat transfer is assessed in the hot exposed tests. Finally, for the water enthalpy variation, an accurate estimation is obtained, as it can be observed in Fig. 10 (C). Errors in the power to water hardly reach values of 200 W. As far as the rotational speed were imposed to be the experimental ones, some energy unbalance is necessarily committed. Fig. 10 (F) shows the energy unbalance made by the model: Turbine mechanical power is being compared against the mechanical losses and compressor consumed mechanical power. If the rotational speed were released, the error in energy balance will be translated into it, being slightly over predicted.

Fig. 11 shows one of the main capabilities of the model: The extrapolated efficiency curves for all three units and 50 % VGT opening. As it can be observed,

regardless of the turbocharger, same conclusions are obtained. Differences between ETE and adiabatic turbine efficiency are very low, and mainly caused by the mechanical losses in the bearings. Fig. 11 also shows for all three units that benchmarking could be done with almost-adiabatic test. However, depending on the required degree of detail (especially at low reduced speed) fully adiabatic results are needed.

Further analysis has been performed for turbo1 and turbo3 to show another example of the model and testing procedure capabilities for benchmarking. Fig. 12 shows for ~50 % VGT position the supplier turbocharger maps. Fig. 12 (A), corresponds to turbo1 and Fig. 12 (B) corresponds to turbo3.

Having considered all the testing boundary conditions, the HT-ML-TCM is employed for the adiabatization and fitting of the supplier maps. Both turbochargers were tested in hot exposed conditions. The most relevant difference between both testing campaigns lies in the cooling water. Turbo1, in Fig. 12 (A) had a given coolant mass flow, while turbo3 Fig. 12 (B) was tested without coolant. ETE definition in Eq. (3) justifies the unrealistic values of the ETE for turbo3. The explanation is the one that follows: Because of the absence of cooling, heat losses from the turbine reach the compressor side, increasing the compressor outlet temperature. In other words, compressor measured power, partially belongs to turbine heat losses, as it is computed as the difference in total enthalpy flow between the compressor outlet and inlet. This effect is more noticeable in the lower speed range, were the heat transfer effects are more significant in relative terms. The maximum difference reaches the value of 28 % between ETE and adiabatized efficiency.

To conclude, adiabatic maps should be the ones used for aerodynamic efficiency comparisons. Otherwise, heat transfer effects, mechanical losses and boundary conditions, hide the actual aerodynamic efficiency of the turbocharger.

5. RESULTS FROM ENGINE TEST SIMULATIONS

Once the models have been validated, an engine experimental campaign has been developed. Full load working points have been tested in the engine. The engine tested speed range covered from 1250 rpm up to 5000 rpm. Turbo1 was coupled to the engine for the experimental in-engine campaign. In addition, these points were simulated in GT-POWER. GT-POWER software was coupled to the calibrated HT-ML-TCM. Results of the simulation and the experimental campaign are shown in Fig. 13. Some key points should be highlighted:

- For each working point simulation, the experimental turbine inlet temperature was imposed. The followed strategy was to set up a PID that controlled the exhaust heat transfer multiplier.
- Experimental Boost pressure is the target for the VGT position.
- Engine speed, AFR, boundary conditions… were imposed.
- Experimental turbocharger lubricant and coolant fluids working conditions were recorded and imposed in the model calculations.
- Blue points in Fig. 13 correspond to the results of the model with the proper water mass flow and inlet temperature. Red working points inFig. 13 correspond to simulations were water was not implemented. The comparison of these two sets of simulations will be the objective of analysis.

As it can be appreciated in Fig. 13 (A), experimental turbine inlet pressure was achieved in any case. The model prediction error for turbine outlet temperature is kept around ±25 ºC depending on the working point, see Fig. 13 (C). Regarding the compressor outlet temperature, in Fig. 13 (E), maximum error hardly reaches 15 ºC in the worst of the cases.

As far as a calibrated heat transfer model was obtained, it was attempted to analyze the effect of cooling water in the turbocharger performance. One could think about a higher available thermal energy for the effective expansion in the rotor if water was not circulated across the housing. Fig. 13 (F) shows that even if cooling water is neglected, the total heat loses power is reduced just around 300 W in average. Heat to the ambient is still important and heat to the oil (mainly) compensates the lack of heat flux to the water. In all, if the turbocharger unit is not actively cooled, the benefit in the brake specific fuel consumption is not noticeable at all. A second indicator that confirms the previous conclusions is the turbine inlet pressure. Regardless of the presence or lack of cooling water, turbine inlet pressure differences are almost undetectable, as it can be seen in Fig. 13 (A). On the contrary, compressor outlet temperature is noticeably affected by the coolant mass flow. Differences go from 1 to 9 ºC from 5000 rpm to 1250 rpm respectively.

Without coolant, oil overheating is obvious. Fig. 14 shows oil outlet temperature for each engine working point. Cooling water is required for oil thermal insulation.

For better understanding of the obtained results, wall temperature distribution has been plotted in Fig. 15. Wall temperature distribution confirms all the previously

stated. In the “non-coolant” configuration, the hotter central housing results in a higher heat flux to the oil and to the compressor. Same happened for turbo3 during the supplier test campaign, as shown in Fig. 12 (B), in which unrealistic values of ETE were resulting from turbine heat reaching the compressor. It is clear that, if water is employed, lower temperature values are achieved in the turbine backplate (H1) and central housing (H2). Thus, an effective protection of the VGT mechanism is accomplished.

6. SUMMARY AND CONCLUSIONS

Heat transfer and mechanical losses have been proved to take an important role in automobile turbochargers. VGT technology is being implemented in small direct injection gasoline engines. In this study, three new generation VGT turbochargers have been studied.

VGT implementation in gasoline engines is possible, among other reasons, thanks to the advanced in materials and active turbine cooling. An active cooling strategy, in combination with the high exhaust gases temperatures (typical in spark ignition engines), motivated this study. A proper calibration of heat transfer and mechanical losses properties becomes of high interest for proper engine simulations.

A carefully designed gas stand experimental procedure and data processing methodology have been disclosed. Different sets of experimental information (adiabatic, hot insulated and hot exposed) were necessary to perform a proper calibration of the HT-ML-TM. The model calibration is constituted by three main steps:

- Almost-adiabatic tests were necessary to provide the turbocharger model with enough data for the aerodynamic maps fitting and extrapolation and for friction losses model calibration. On the one hand, if almost-adiabatic data is pretended to be directly used as the turbocharger maps, special care should be taken with the stabilization criteria. It would be preferable to wait until all the mean working fluids temperatures are totally stabilized. On the other hand, if it is possible to adiabatize the experimental data, stabilization criteria could be applied only to: turbine inlet, oil inlet and compressor outlet. For this study, both approaches were followed. From mean fluids temperature stabilization approach, better stabilization was achieved. The last was concluded during the energy balance study. However, it was also proved that the differences in the adiabatization process were hard to find between both experimental procedures.
- Hot insulated cases allowed for the internal heat transfer model calibration.
- Hot exposed tests, which allowed for external heat transfer model calibration.

Having obtained the purely adiabatic maps, a turbocharger benchmarking can be properly done, as it is shown for the studied turbocharger units.

Maps tested at very different conditions (with and without water cooling) were compared. The processing of these maps reflected the necessity of adiabatizing hot maps if a turbochargers benchmarking is aimed. It was also evidenced the affection of the boundary conditions in the hot maps. In the case of hot maps without cooling water

(supplier turbo2), ETE values in low power points are mostly governed by heat transfer, rather than aerodynamics.

Turbo1 was assembled in a gasoline EU6 engine. Nine full load working points (1250-5000 rpm) were tested and also simulated in GT-POWER. In GT-POWER simulations, experimental inlet turbine temperature was ensured by means of a PID. Also, the developed and calibrated turbocharger model for turbo1, was coupled into GT-POWER. Experimental inlet coolant and oil temperatures (and mass flows) were imposed during the simulation campaign. VGT mechanism during the simulations pursued the experimental boost pressure, and the experimental AFR ratio were imposed.

Good agreement was obtained between the experimental engine data and simulation campaigns. This was after performing the outsourced calibration procedure of the turbocharger model, relaying just on gas stand data, and without needing further calibration of the turbocharger efficiency in GT-POWER. BSFC and turbine inlet pressure were properly predicted. The relative error in the BSFC oscillated within the range of 0.7-3.1 %.

A second set of simulations was performed without the experimental cooling water mass flow of the turbocharger, in order to assess modelling procedure sensibility to engine operative conditions. Heat to the ambient and to the lubricating oil compensates the lack of cooling media. Main engine output variables are not affected by the lack of water. In all, avoiding water cooling the turbocharger does not present any positive impact neither in the turbocharger nor in the engine performance.

Furthermore, it has been demonstrated the necessity of water for avoiding oil coking. Without cooling water, oil temperature reached values of 175ºC. Compressor outlet temperature can be affected in a noticeable way by the absence of cooling water, with differences reaching 10ºC in some cases. Finally, regarding the VGT mechanism protection, if water coolant is used, wall temperature is lowered around 100ºC in the central housing, and 70ºC in the turbine backplate.

ACKNOWLEDGMENT

The authors wish to thank M.A. Ortiz, R. Carrascosa and Valentín Ucedo for their invaluable work during the experimental setup and campaign in the gas stand test bench.

FUNDING

Alejandro Gómez Vilanova is partially supported through contract Subprograma 1 (PAID-01-18) of Universitat Politècnica de València. This work was partially funded ayuda a Primeros Proyectos de Investigación (PAID-06-18), Vicerrectorado de Investigación, Innovación y Transferencia of Universitat Politècnica de València.

NOMENCLATURE

AFR	Air Fuel Ratio
A_{i}	External area of node “i” (m^2)
BSFC	Break Specific Fuel Consumption (g/Kw-h)
$K_{i-(1+1)}$	Metal Thermal conductance (W/K)
ETE	Effective Turbocharger Efficiency

HT	Heat Transfer
HTM	Heat Transfer Multiplier
$h_{\mathrm{i-ext}}$	External convective coefficient of node “i”
h_{jb}	Clearance of the journal bearing
K_{jb}	Journal Bearings correcting factor
L_{JB}	Length of the journal bearing
ML	Mechanical Losses
n	Turbocharger shaft rotational speed
R_{JB}	Radius of the journal bearing
SRCT	Self-Recirculation Casing Treatment
T_i	Temperature of element “i”
VGT	Variable Geometry Turbine
WG	Waste-Gate
$\dot{W}$	Power
ε	Square Mean Root Error
μ	Viscosity

REFERENCES

[1] Zeppei D, Koch S, Rohi A. Ball Bearing Technology for Passenger Car Turbochargers. Motortechnische Zeitschrift - Springer 2016;77:26–31.

[2] Galindo J, Serrano JR, Climent H, Varnier O. Impact of two-stage turbocharging architectures on pumping losses of automotive engines based on an analytical model. Energy Conversion and Management 2010;51:1958–69. https://doi.org/10.1016/j.enconman.2010.02.028.

[3] Avola C, Copeland C, Duda T, Burke R, Akehurst S, Brace C. Review of Turbocharger Mapping and 1D Modelling Inaccuracies with Specific Focus on Two-Stage Systems 2015. https://doi.org/10.4271/2015-24-2523.
[4] Mingyang Y, Ricardo M botas, Kangyao D, Yangjun Z, Xinqian Z. Unsteady influence of Self Recirculation Casing Treatment (SRCT) on high pressure ratio centrifugal compressor. International Journal of Heat and Fluid Flow 2016;58:19–29. https://doi.org/10.1016/j.ijheatfluidflow.2015.12.004.
[5] Zheng X, Zhang Y, Yang M, Bamba T, Tamaki H. Stability Improvement of High-Pressure-Ratio Turbocharger Centrifugal Compressor by Asymmetrical Flow Control—Part II: Nonaxisymmetrical Self-Recirculation Casing Treatment. Journal of Turbomachinery 2012;135:021007. https://doi.org/10.1115/1.4006637.
[6] Chiong MS, Rajoo S, Martinez-Botas RF, Costall AW. Engine turbocharger performance prediction: One-dimensional modeling of a twin entry turbine. Energy Conversion and Management 2012;57:68–78. https://doi.org/10.1016/j.enconman.2011.12.001.
[7] C.D. Rakopoulos., E.G. Giakoumis. “Diesel Engine Transient Operation.” Springer; 2009.
[8] Serrano JR, Olmeda P, Arnau FJ, Dombrovsky A, Smith L. Turbocharger heat transfer and mechanical losses influence in predicting engines performance by using one-dimensional simulation codes. Energy 2015;86:204–18. https://doi.org/10.1016/j.energy.2015.03.130.
[9] Serrano J, Olmeda P, Arnau F, Reyes-Belmonte M, Lefebvre A. Importance of Heat Transfer Phenomena in Small Turbochargers for Passenger Car Applications. SAE International Journal of Engines 2013;6:716–28. https://doi.org/10.4271/2013-01-0576.
[10] Marelli S, Marmorato G, Capobianco M, Rinaldi A. Heat Transfer Effects on Performance Map of a Turbocharger Compressor for Automotive Application. SAE Technical Paper 2015. https://doi.org/10.4271/2015-01-1287.
[11] Payri F, Olmeda P, Arnau FJ, Dombrovsky A, Smith L. External heat losses in small turbochargers: Model and experiments. Energy 2014;71:534–46. https://doi.org/10.1016/j.energy.2014.04.096.
[12] Serrano JR, Olmeda P, Arnau FJ, Reyes-Belmonte MA, Tartoussi H. A study on the internal convection in small turbochargers. Proposal of heat transfer convective coefficients. Applied Thermal Engineering 2015;89:587–99. https://doi.org/10.1016/j.applthermaleng.2015.06.053.
[13] Serrano JR, Olmeda P, Tiseira A, García-Cuevas LM, Lefebvre A. Theoretical and experimental study of mechanical losses in automotive turbochargers. Energy 2013;55:888–98. https://doi.org/10.1016/j.energy.2013.04.042.
[14] Society of Automotive Engineers. Supercharger Testing Standard. SAE Vehicle Standard 1995:1–9. https://doi.org/J1723_199508.
[15] Serrano JR, Olmeda P, Arnau FJ, Samala V. A holistic methodology to correct heat transfer and bearing friction losses from hot turbocharger maps in order to obtain adiabatic efficiency of the turbomachinery. International Journal of Engine Research 2019:146808741983419. https://doi.org/10.1177/1468087419834194.

[16] Serrano JR, Arnau FJ, García-Cuevas LM, Dombrovsky A, Tartoussi H. Development and validation of a radial turbine efficiency and mass flow model at design and off-design conditions. Energy Conversion and Management 2016;128:281–93. https://doi.org/10.1016/j.enconman.2016.09.032.

[17] Payri F, Serrano JR, Fajardo P, Reyes-Belmonte MA, Gozalbo-Belles R. A physically based methodology to extrapolate performance maps of radial turbines. Energy Conversion and Management 2012;55:149–63. https://doi.org/10.1016/j.enconman.2011.11.003.

Figure Captions List

Fig. 1 Gas stand in insulated configuration

Fig. 2 Gas stand in exposed configuration

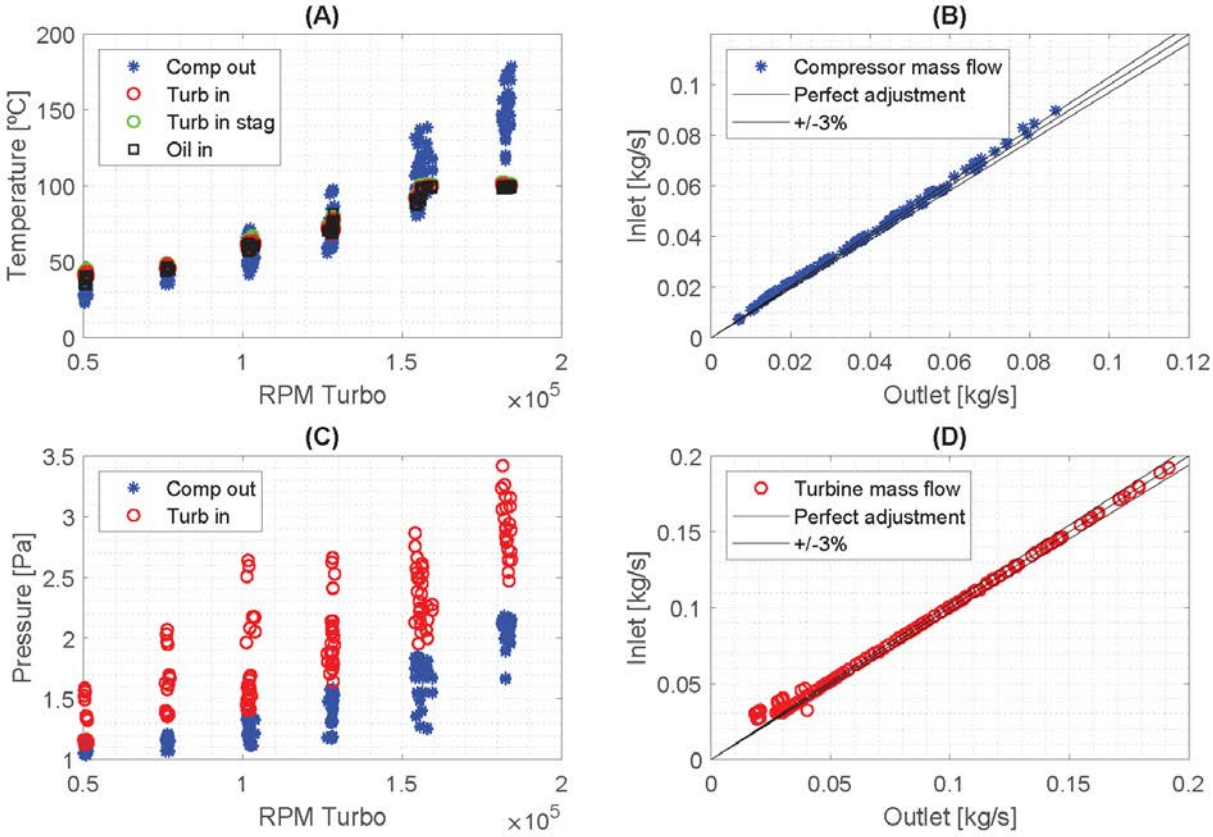

Fig. 3 Recorded variables under almost-adiabatic conditions

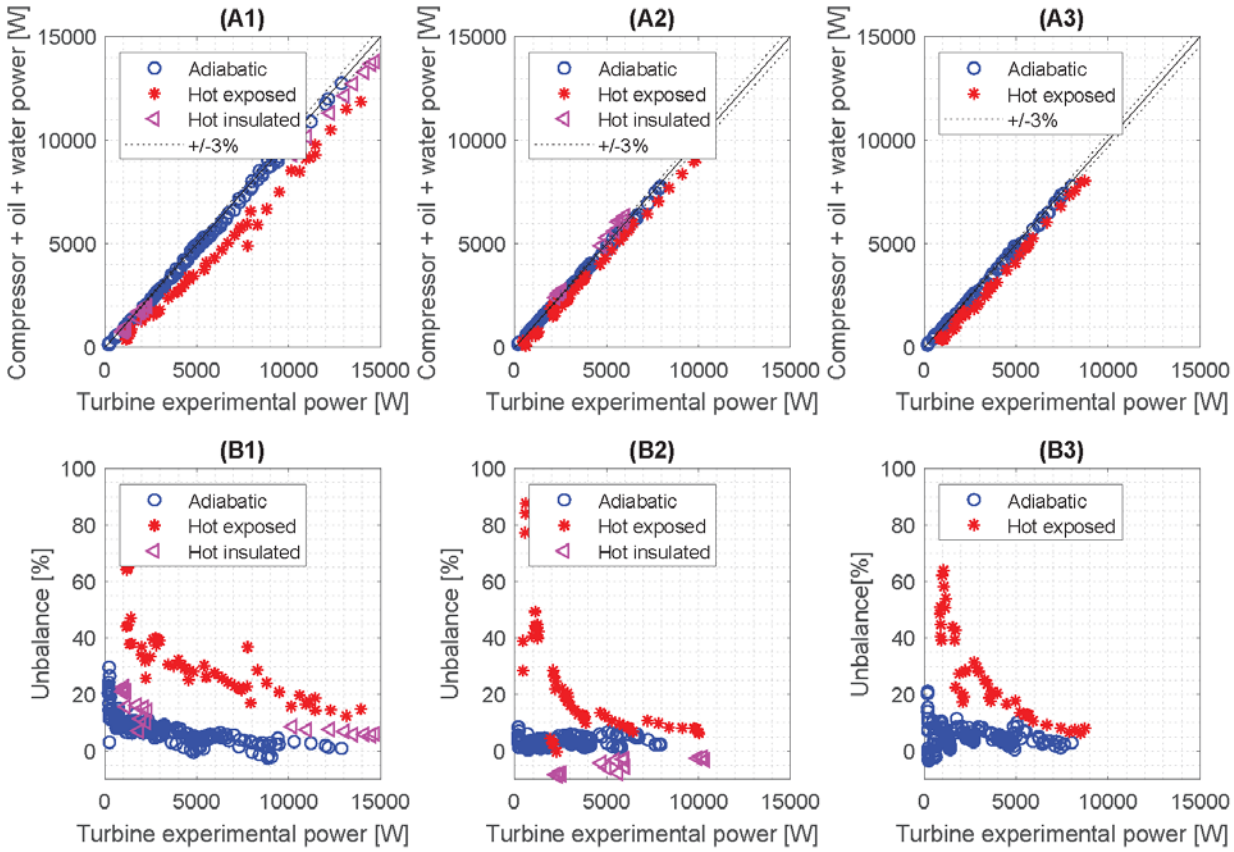

Fig. 4 Energy balance. Turbo1: (A1), (B1). Turbo2: (A2), (B2). Turbo3 (A3), (B3)

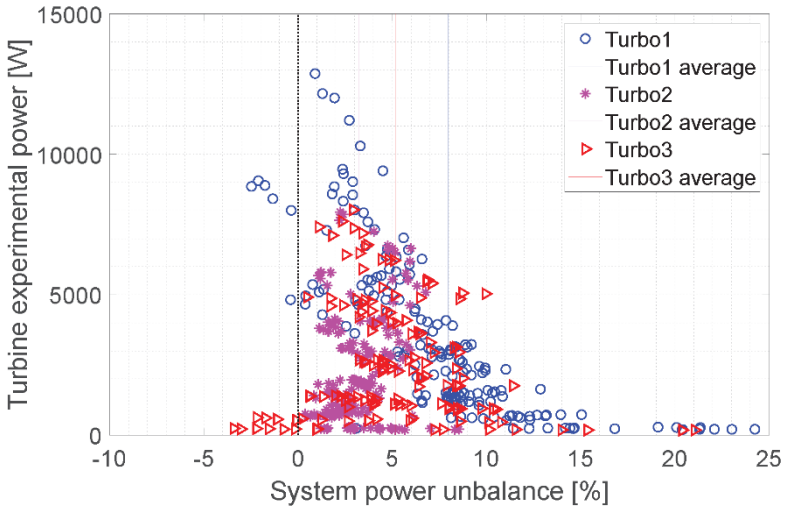

Fig. 5 Adiabatic test unbalance for turbo1, turbo2 and turbo3

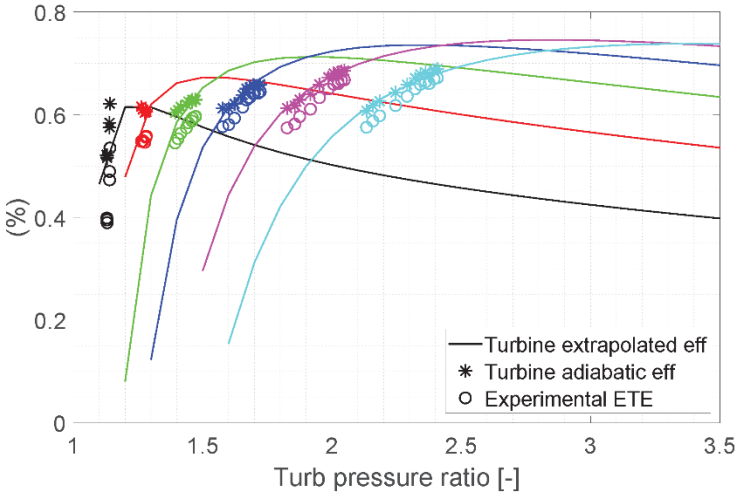

Fig. 6 Turbo1, 50 % VGT, experimental ETE, adiabatized efficiency and fitted-extrapolated efficiency

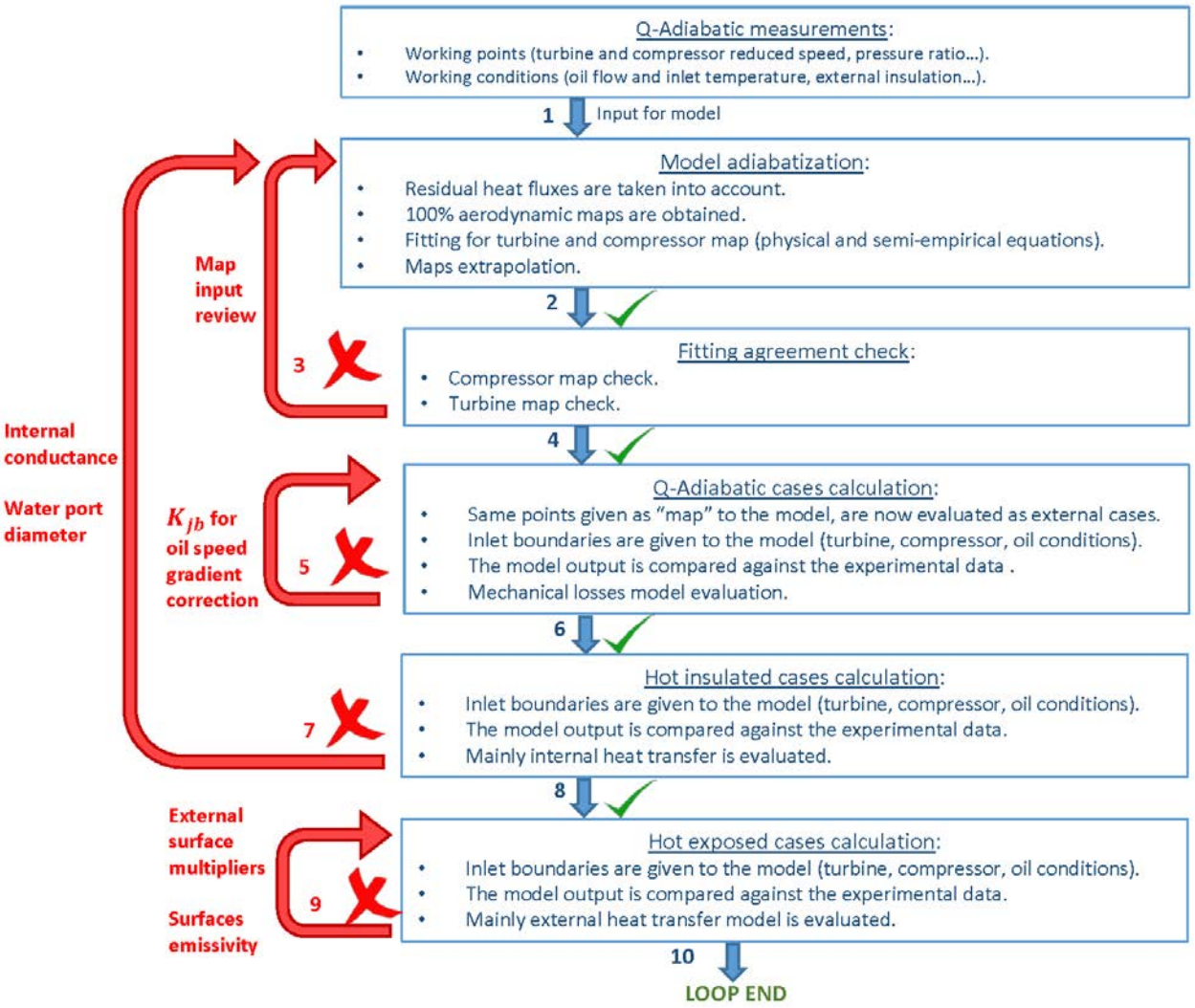

Fig. 7 Diagram for HT-ML-TCM calibration procedure

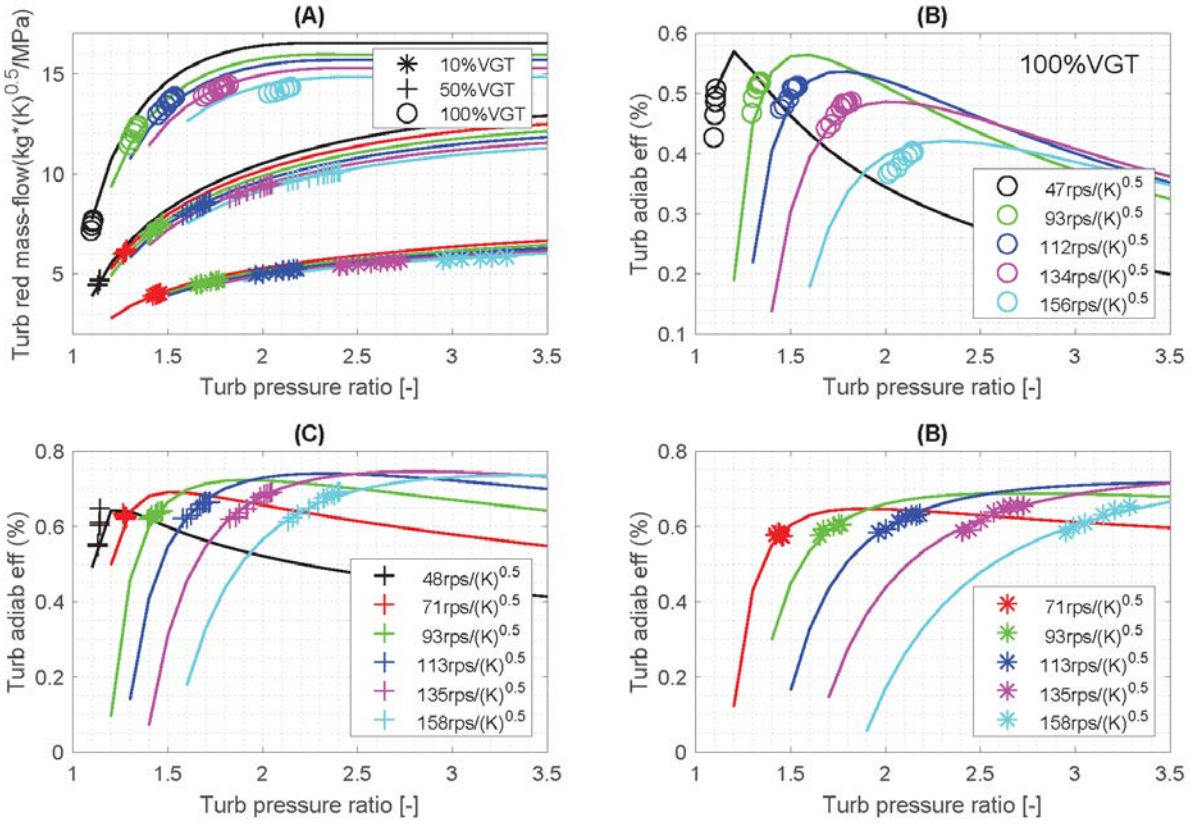

Fig. 8 Turbo1 obtained maps

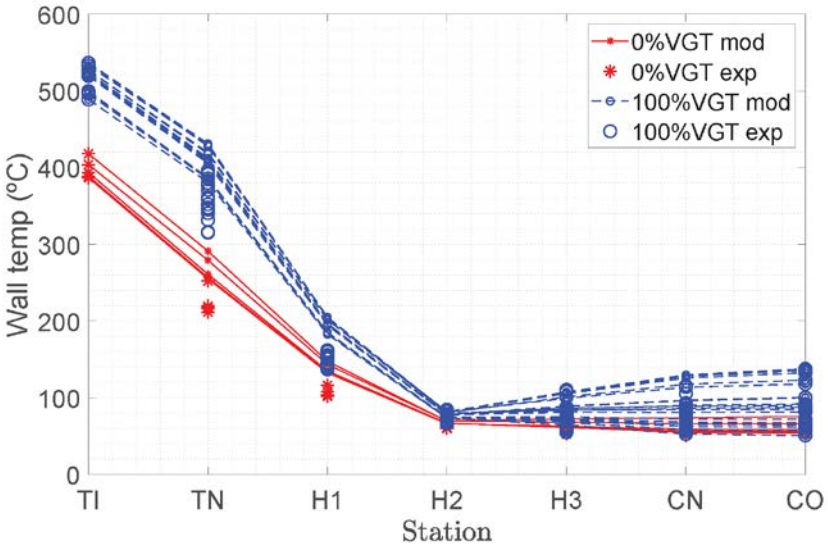

Fig. 9 Hot exposed simulations VS experiments. Turbo1, wall temperature distribution

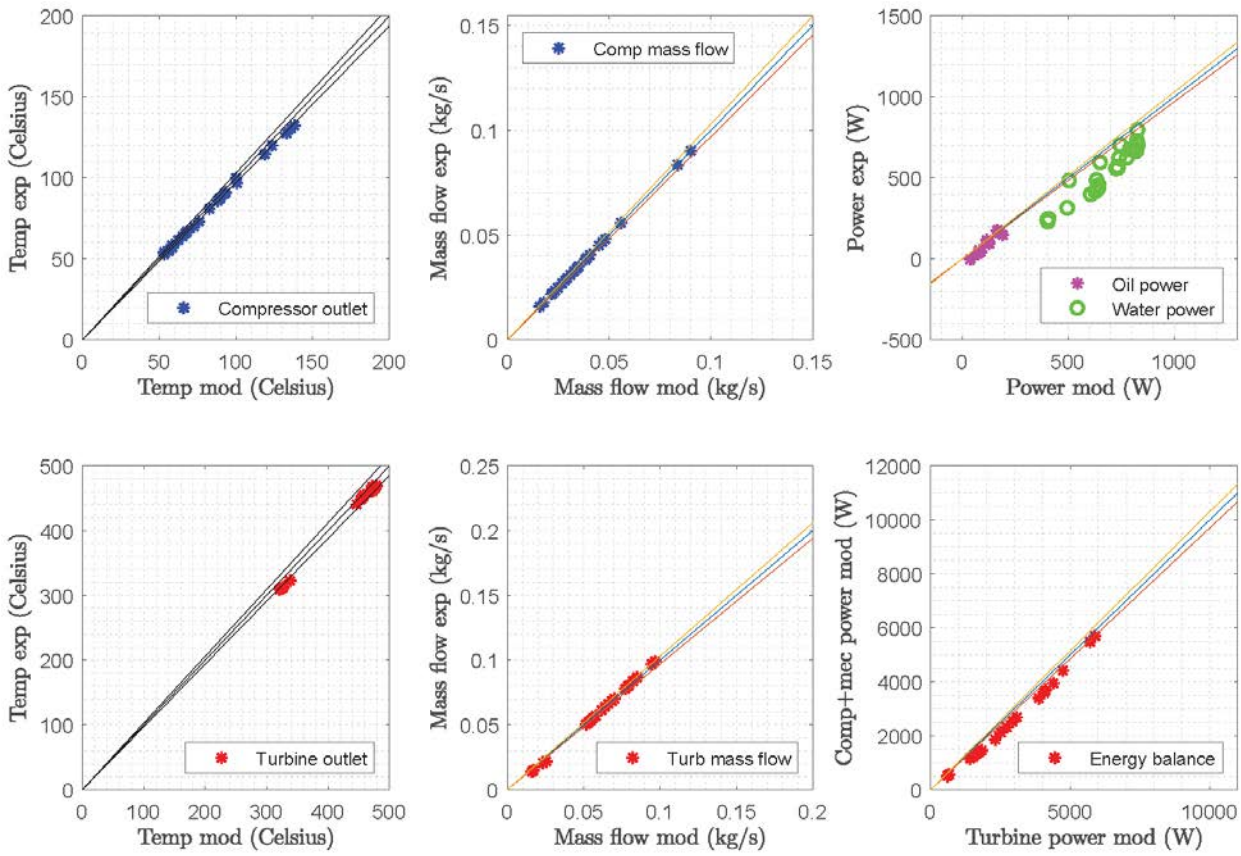

Fig. 10 Hot exposed cases: Simulations VS experiments for Turbo1

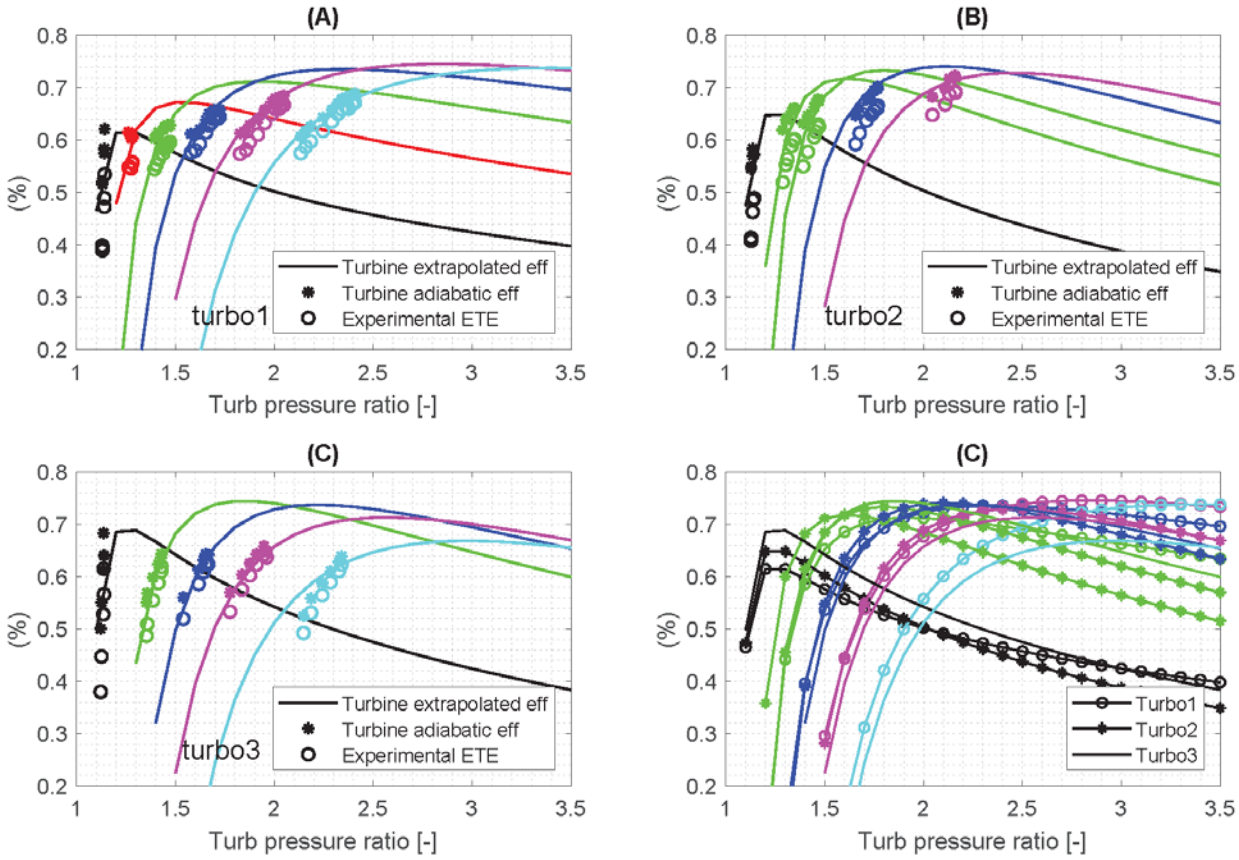

Fig. 11 Turbochargers adiabatization, fitting, extrapolation and benchmarking for 50 % VGT opening. Turbo1 (A), turbo2 (B), turbo3(C), comparison (D)

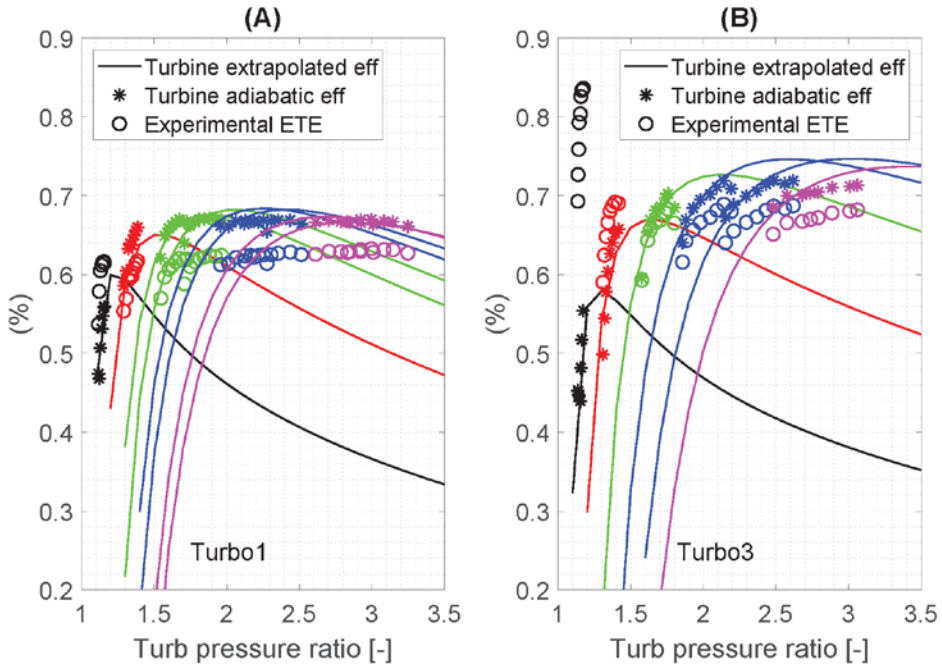

Fig. 12 Supplier hot maps, including model adiabatization and extrapolation. (A) Corresponds to turbo1. (B) Corresponds to turbo3

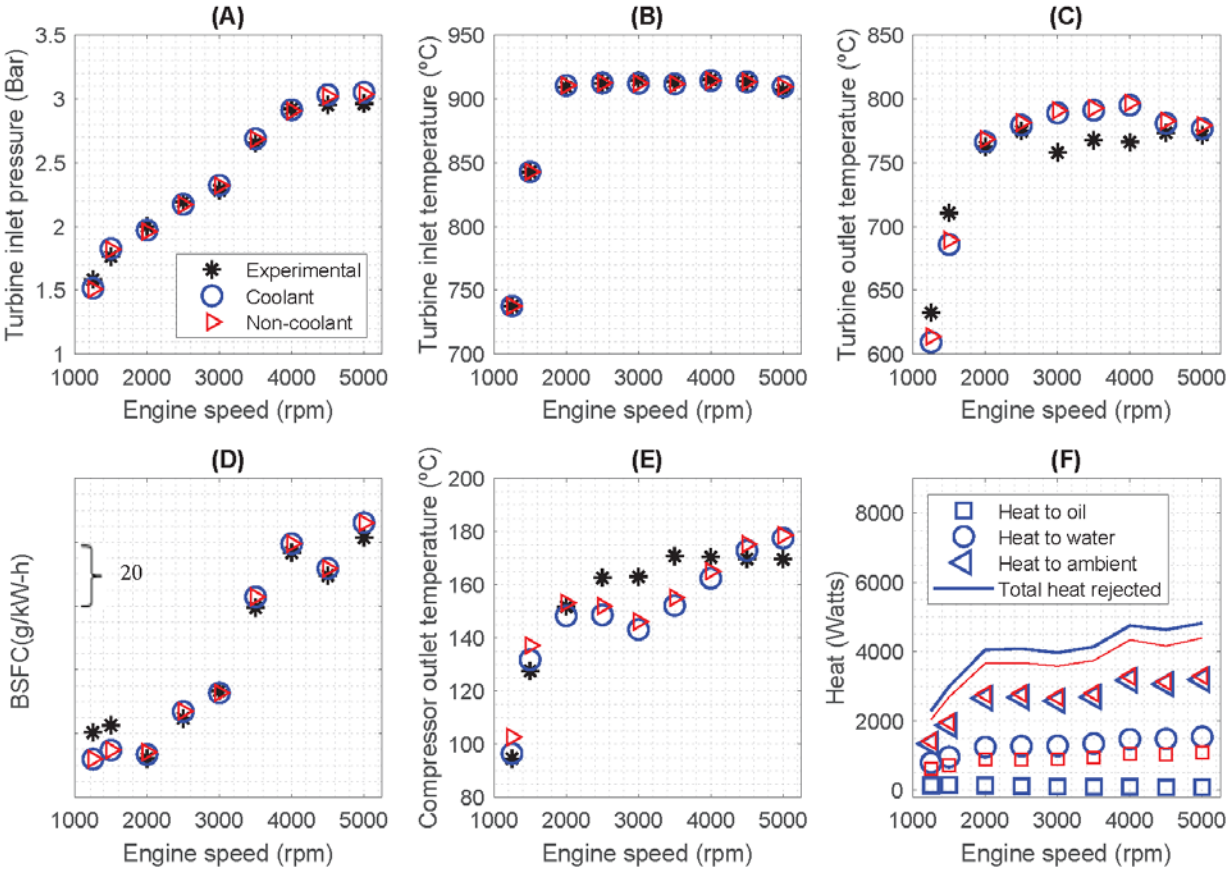

Fig. 13 Full load engine simulations. Model VS experimental campaign

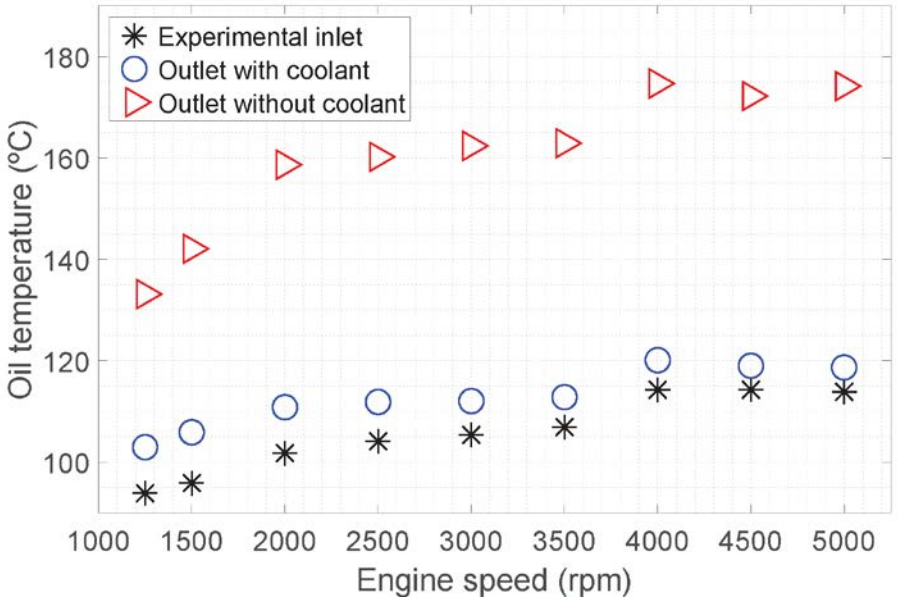

Fig. 14 Results from engine simulations. Oil temperature evolution w/o cooling water

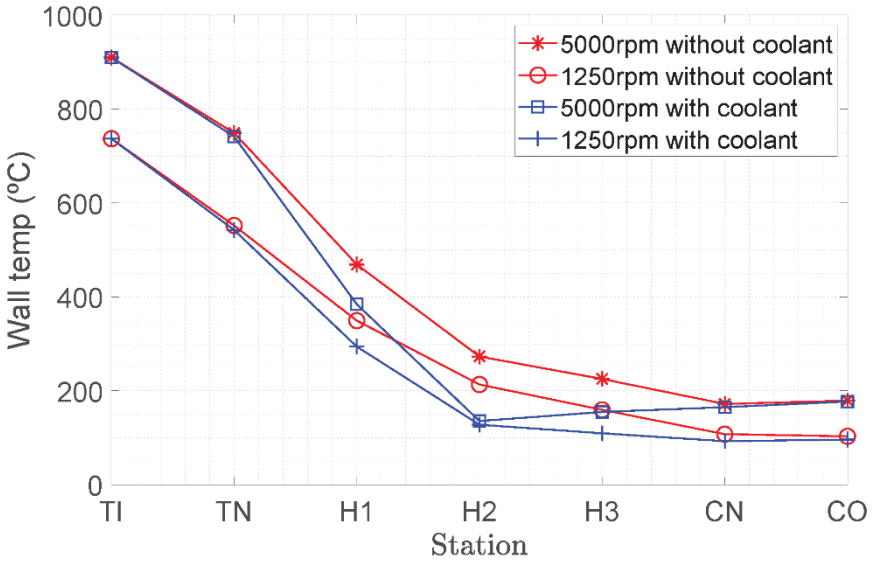

Fig. 15 Turbo wall temperature distribution. 1250 and 5000 engine rpm

Table Caption List

Table 1 Iso-speed range-color criteria for turbine maps

colour	Speed range [rps/sqr(K)]
black	]0, 50]
red	]50, 75]
green	]75, 100]
blue	]100, 125]
magenta	]125, 150]
cyan	]150, 160]

Table 2 Mass flow and efficiency mean square root errors

turbo1		turbo2		turbo3	
ε mass	ε eff	ε mass	ε eff	ε mass	ε eff
0.88%	0.67%	0.25%	0.49%	0.22%	0.75%